

OPTIMAL PARAMETER SELECTION-BASED DEEP SEMI-SUPERVISED GENERATIVE LEARNING AND CNN FOR OVARIAN CANCER CLASSIFICATION

Pillai Honey Nagarajan and N. Tajunisha

Department of Computer Science, Sri Ramakrishna College of Arts and Science for Women, India

Abstract

A segmentation and categorization of ovarian cancer varieties from Computed Tomography (CT) scans is greatly necessary in current medicinal diagnosis system to lessen the mortality rate. To perform this task, a Deep Semi-Supervised Generative Learning with Enhanced U-Net and fused Deep Convolutional Neural Network (DSSGL-EUNet-DCNN) was developed to augment the training ovarian CT scans, partition the Region-Of-Interests (ROIs), and classify the varieties of ovarian cancer. But, its efficiency depends on the selection of hyperparameters for learning the deep learner. Hence in this article, a DSSGL-EUNet with Multi-Scale DCNN (DSSGL-EUNet-MSDCNN) model is proposed which contains different kernel sizes, learning rate and batch size for multiple DCNN to classify the types of ovarian cancers. First, the training CT scans are augmented by the DSSGL and the ROIs from each CT scan are segmented by the EUNet models. Then, the segmented ROIs are fed to the fused DCNN structure in which every DCNN captures the features from each segment at a scale-level. Also, the hyperparameters of DCNNs are chosen by the lion optimization algorithm for feature extraction and classification. Based on this process, the training errors and time cost are reduced with high classification accuracy. At last, the experimental results exhibit that the DSSGL-EUNet-MSDCNN realizes a higher accuracy than the classical models for segmentation and classification of ovarian cancers.

Keywords:

Ovarian Cancer Types, DSSGL-DCNN, EUNet Segmentation, Multi-Scale Deep Learning, Hyperparameter Optimization, Lion Optimization

1. INTRODUCTION

The tumor is a pathogenic disease that causes unmonitored cell growth to disperse into more organisms. It reflects a wide scope of pathologies including a deadly illness. Cancer cells is not connected with a particular organ, rather, it begins as an unpredictable collection of the cell membrane and spreads throughout the body while cancer cells reproduce and move into the blood vessels. The better way is that a few tissues are less structured than immune tissues if they're not appropriately activated. The processing of a particular protein either an antibody or a functional product by using a DNA-coded gene is often known as genetic information [1].

The control of phenotypic recurrence contributes greatly to cell function preservation. The most familiar example of gynaecological disease among numerous diseases is ovarian tumor [2]. The incidence among gynaecological pathogens is significantly higher since most tumors are diagnosed especially early. Also, reliable treatment is applied to diagnose tissues and organs of the tumor in the removal of primary ovarian tumor tissues to promote better quality of life after treatment. In contrast, the initial diagnosis is very difficult and prone to training discrepancies.

An unpredictable biopsy of the cells has been clearly defined from this perspective. Morphological and neurological testing is initially performed. All such testing will be carried out in varying circumstances in order to resolve discrepancies, but failures are still exist [3]. The most reliable method to lessen the incidence of tumor is to recognize it faster. A diverse variety of operative research findings and ovarian tumor diagnostic datasets are likely to be found. The use of different medical images and classification algorithms to develop a surgical test has been investigated in biomedical application for supporting early identification by many clinicians [4]. Combination of images produced using multiple imaging analytical tools and highly developed technologies in radiography to ensure the efficiency of the taxonomy of ovarian tumours.

Deep Neural Networks (DNNs) using CT images are particularly essential in assisting treatments to be incredibly beneficial and lowering casualty and pharmacologic failures [5]. The important strength of wide knowledge is a lot of information that selects skilled facilities and opportunities. CT images include a numerous advantage such as pervasive use, improved quality, lower cost and quick imaging time. The quantification and prediction of ovarian tumours in standard treatments is therefore subject to CT scans. The differentiation and diagnosis of several illnesses is popularly reported by CNN through CT scans which include the brain, liver, skin cells, and so on [6]. Nonetheless, the ovarian tumor cannot be detected and treated by CT scans within a proper classifier. For this purpose, the CT scan dataset was processed in the form of a DCNN structure relying on AlexNet for the categorization of ovary tumors. This design incorporates 5 convolutional, 3 max-pooling, and 2 reconnect units. In contrast, its precision was not very satisfactory. As a result, DCNN structure relying on the integration of AlexNet, VGG and GoogLeNet [7] has been designed. In this design, the integration was done at the last softmax layer and the scores of the softmax layers of every structure were aggregated by the weighted sum to get the ovarian tumor kinds.

On the contrary, overfitting was occurred if the quantity of learning scans was not adequate. So, a DSSGL-DCNN model was developed depending on the Generative Adversarial Network (GAN) as an image augmentation scheme. But the training images were directly given to this model which tends to high training time. So, a segmentation scheme was employed in this model depending on U-Net structure [8] to split the ROIs from the CT images. It was a pixel-to-pixel, end-to-end fully convolutional engaging skip layers between analysis and synthesis links. Conversely, it includes only some layers and thus it was not adequately effective for partition.

For that reason, a EUNet structure [9] has been designed with the DSSGL-DCNN model to improve the segmentation and categorization efficiency. This EUNet includes the analysis and synthesis links. Every link has inception-res unit, the dense-

inception unit, the downsampling and the upsampling units for producing the feature-level partitioned maps of the CT images. The inception-res unit was utilized to extend the network width via fine-tuning the typical convolutional layers. The dense-inception unit was utilized to extract the features in ROIs and construct the network more deep without additional training variables. The downsampling was utilized to lessen the size of feature maps and learning time. The upsampling unit was used to resize the partitioned feature maps. If the growth rate in the dense-inception unit was increased, then it may use multiple variables which create a highly complicated training. To solve this problem, the feature-level possibility map was produced which was thresholded to binary and merged with the feature-level partitioned maps for generating the discriminative partitioned image. This final partitioned image was given to the DCNN relying on integrated structure for recognizing the ovarian tumor categories. On the other hand, its classification accuracy depends on the choice of hyperparameters for DCNN training which adjusts the hyperparameter ranges and minimizes the learning errors. The considered hyperparameters include the count of units, batch dimension, weights and dropout percentage. The assignment of DCNN hyperparameters is difficult process. The standard optimization algorithms cannot adjust the hyperparameter ranges within the model structure.

Therefore, this paper introduces a MS-DSSGL-EUNet-DCNN model for segmenting and classifying the types of ovarian cancers. This model considers different kernel sizes, learning rate and batch size for multiple DCNNs. In this model, the ROIs from each CT scan are given to the fused DCNN model wherein each DCNN extracts the features from all segments at a scale-level. Also, the DCNN hyperparameters such as the number of layers, kernel sizes, learning rate, batch size, weights, and dropout rate are optimized by the lion optimization algorithm. This can reduce the training errors and training time effectively. So, the accuracy of segmenting and categorizing the ovarian tumor categories is increased.

The remaining article is prepared as the following: Section 2 studies various deep learner models for categorizing different diseases using different imaging modalities. Section 3 explains the functioning of proposed model and Section 4 demonstrates its efficiency. Section 5 gives the conclusion and future scope to this research.

2. LITERATURE SURVEY

A new completely automated method [10] has been developed which uses the CNN integrated with the graph-cuts optimization for differentiating the arteries and veins in lung CT scans. Initially, the pulmonary area from the lung CT scan and the vessels were partitioned by the scale-space particles method for representing the vessel candidates. After that, the CNN was learned by the extracted 3D patches. The CNN hyperparameters were optimized by the graph-cuts optimization to train the closeness of arteries to veins. But, it may be biased toward creating a small contour because of obtaining the minimum cut.

A 3D Gray-Level Co-occurrence Matrix based CNN (3D-GLCM-CNN) [11] has been developed to recognize polyp from CT scans. First, the raw CT range of the 3D polyp was transformed into the gray-scale depending on the CT range

allocation of the entire corpus. Then, many 3D-GLCM scans were created from the gray-scale scans acquired from the primary phase. Further, a multi-channel CNN was applied for classifying the polyp utilizing the GLCM feature scans. But, it needs additional features and hyperparameter tuning for increasing the accuracy.

Grid Search-based Hyper-Parameter Tuning (GSHPT) [12] has been suggested for random forest variables to categorize the microarray tumor information. In this approach, the optimal variables were found which offer the highest number of features for partitioning the node, amount of decision trees in a forest, depth of the trees and condition to partition a node into the child node. Also, the out-of-bag loss was used to verify the optimized variables which tend to the better efficiency. But, there was no promise that this approach can provide the better solution.

A technique [13] has been developed for a single-scan super-resolution 3D CT images depending on the DCNNs with 10 convolutional units and an transitional upscaling unit. The primary and secondary CNNs were used for enhancing the resolution on 2D and 3D axes, respectively. Also, the loss concerning the ground-truth super-resolution scan followed by the upscaling unit was determined with the loss after the final convolutional layer. As well, a Gaussian smoothing with different standard variances was applied for preventing overfitting. But, it needs to optimize the hyperparameters for increasing the efficiency.

Multi-task Multi-scale deep learner System called M3Lung-Sys [14] has been designed by considering slice- and patient-level CNNs for multi-class pulmonary pneumonia prediction from CT scans. First, the pulmonary CT scans were collected and pre-processing was done to remove the noise or unwanted features from the scans. Then, a hand-crafted method was used to partition the images into pulmonary and other. Also, the least bounding rectangle within a given edge was used to crop the pulmonary region. Further, the slices were given to the DCNNs for predicting different disorders: COVID-19, H1N1, pneumonia, and healthy people. However, it may still miscategorize few healthy people and also it was not end-to-end learnable which may cause the visualization of unique lesion's distributions for every disorder automatically.

An Evolutionary multi-objective optimization Based Tool (EBST) [15] has been designed to find microRNAs with promising biomarkers in ovarian tumor. At first, the serum microRNA profiles were collected and the Fisher Discriminant Ratio (FDR) filtering was done as pre-processing. Then, modified multi-objective imperialist competitive algorithm was used to choose the relevant feature subsets by optimizing multiple objective functions. Further, the l₁-Support Vector Machine (SVM) classifier has been applied to categorize the chosen features. On the other hand, it needs to select the appropriate kernel functions of SVM to achieve better efficiency.

An integrated method [16] has been developed to choose the features and categorize the ovarian tumor. First, the features were chosen by the different chromosome choice schemes: relationship coefficient, T-statistics and Kruskal-Wallis trial. Then, the chosen characteristics were adopted using the central force adaptation, lighting addition process adaptation, genetic bee colony optimization and artificial algae optimization. Further, the optimized features were categorized with the different classifiers:

Linear Discriminant Analysis (LDA), K-Nearest Neighbor (KNN), Logistic Regression (LR), SVM with RBF kernel, and Multi-Layer Perceptron (MLP). But, these classifiers have less accuracy and high training time for large-scale datasets.

3. PROPOSED METHODOLOGY

In this section, the DSSGL-EUNet-MSDCNN model is explained briefly. The Fig.1 depicts the schematic overview of this model for ovarian cancer categorization.

The main processes in this model are the following:

- Initially, the training CT scans are collected and augmented by the DSSGL model.
- After, those augmented scans are fed to the EUNet for partitioning the ROIs from ovarian tumor CT scans.
- Then, these segmented ROIs are given to the MS-DCNN fused structure in which the lion optimization algorithm is performed to choose the optimal hyperparameters of each network structure for extracting and classifying the ovarian tumor types.

3.1 IMAGE COLLECTION AND SEGMENTATION

First, the ovarian tumor CT scans are acquired from The Cancer Genome Atlas-Ovarian (TCGA-OV) corpus, which covers the 43 ovarian tumor CT scans in DICOM form. Such CT scans are augmented by the DSSGL model to extend the number of training images [7]. Thus, it creates an overall of 497 scans for 7 classes of ovarian tumors: ovarian epithelial tumor, germ cell tumors, sex cord-stromal tumors, serous carcinoma, mucinous carcinoma, endometrioid carcinoma and clear cell carcinoma. Afterward, the learning images are provided to the EUNet model to split the desired ROIs [9]. By training the EUNet model, the feature-level segmented maps and probability maps are produced. Also, these 2 different maps are merged to obtain the resultant discriminative segmented feature maps.

3.2 OPTIMAL HYPERPARAMETER SELECTION USING LION OPTIMIZATION ALGORITHM FOR FUSED MULTI-SCALE DCNN-BASED CATEGORIZATION

After segmentation, the MSDCNN is employed for classification task based on fused structures: AlexNet, VGG16, and GoogLeNet. In this MSDCNN, the hyperparameters include the number of layers (L), learning rate (α), dropout rate (τ), weight values (w), and kernel sizes (k) are optimized by the lion optimization algorithm for reducing the training errors. The major processes in lion optimization algorithm are described below.

Initialization

Originally, the population is generated in a random manner over the search space. All outcomes are called lion (each network structure in the MSDCNN model). In a d -dimensional optimization dilemma i.e., d set of hyperparameters: L, α, τ, w , and k , a lion (network structures in the MSDCNN) is represented by Eq.(1)

$$Lion(MSDCNN) = [l_1, \dots, l_d] \quad (1)$$

The fitness (classification accuracy) of MSDCNN structure (lion) is computed as Eq.(2).

$$f(MSDCNN) = \max accuracy = f(l_1, \dots, l_d) \quad (2)$$

In the starting step, d_{pop} outcomes are produced arbitrarily in hunt space, % d of produced outcomes is arbitrarily decided as MSDCNN structures: AlexNet, VGG16, and GoogLeNet. The residual inhabitants are separated arbitrarily into φ prides. All outcomes have a particular sex and keep fixed. At the searching procedure, all lions monitor their best entered locality to generate an area. So, for all prides, monitored localities (optimal entered localities) using their associates create that pride's area.

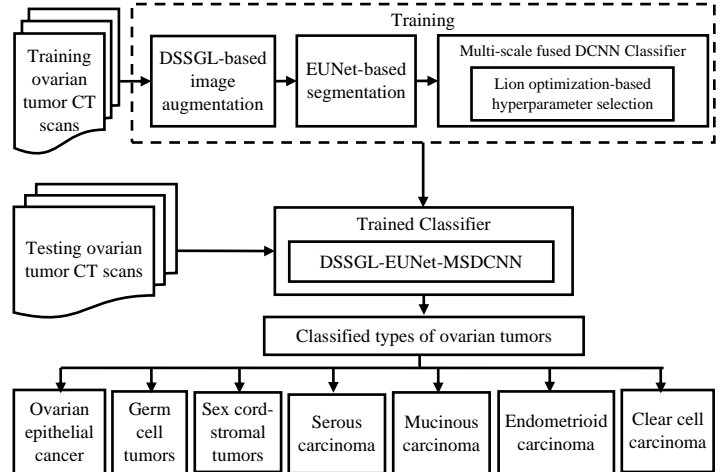


Fig.1. Schematic Overview of DSSGL-EUNet-MSDCNN Model for Ovarian Tumor Segmentation and Categorization

Hunting

In each pride, a number of female concentrates on a victim (optimal set of L, α, τ, w , and k) in a crowd to give a food for their pride. Such seekers comprise certain mechanisms to surround the victim and preserve it. Typically, MSDCNN pursued about equal structures in hunting. All lions fine-tune its locality relying on their specific locality and the localities of group associates. Because of this idea that in searching several such seekers surrounds victim and assaults from conflicting locality, opponent-related training is applied.

So, the seekers are separated into 3 subgroups arbitrarily. Crowd with the peak fitness of associates is called a centroid and the remaining 2 groups are called 2 wings. A false victim (prey) is engaged in the centroid of seekers ($prey = \sum hunters(l_1, \dots, l_d) / \text{number of hunters}$). At hunting, seekers are decided in sequence, and all decided seekers assault on false victim in accordance with the crowd that decided lion is belonging to that. If a seeker improved its fitness, prey will get away from seeker and fresh locality of prey ($prey'$) is discovered as:

$$prey' = prey + \text{rand}(0,1) \times PI \times (prey - \text{hunter}) \quad (3)$$

In Eq.(3), prey is the present locality of victim, hunter is the present locality seeker who hit to victim and PI indicates the rate of increase in objective of seeker. To imitate encircling victim by the decided seeker crowds, the fresh localities of seekers ($hunter'$) belonging to the left and right wings are generated by:

$$hunter' = \begin{cases} \text{rand}((2 \times prey - \text{hunter}), prey) & \text{if } (2 \times prey - \text{hunter}) < pr \\ \text{rand}(prey, (2 \times prey - \text{hunter})) & \text{if } (2 \times prey - \text{hunter}) > pr \end{cases} \quad (4)$$

In addition to this, the fresh localities of centroid seekers are produced as:

$$hunter' = \begin{cases} rand(hunter, prey) & \text{if } (2 \times prey - hunter) < pr \\ rand(pre, hunter) & \text{if } (2 \times prey - hunter) > pr \end{cases} \quad (5)$$

In Eq.(4) and Eq.(5) $rand(a,b)$ produces an arbitrary value from a to b which are upper and lower limits, respectively.

Shifting towards Secure Site

The fresh locality for a female lion is described by

$$female\ lion' = female\ lion + 2Dist \times rand(0,1)\{R1\} + U(-1,1) \times \tan \theta \times Dist \times \{R2\} \{R1\} \cdot \{R2\} = 0 \parallel \{R2\} \} = 1 \quad (6)$$

In Eq.(6), female lion is the present location of female lion, Dist is the gap amid the female lion’s locality and the spot decided using the event choice amid the pride’s region, {R1} refers to the vector that its initial locality is the earlier locality of the female lion and its path is toward the decided locality, {R2} refers to the perpendicular to {R1}. The victory of a lion is expected when it increases his/her optimal locality at the final iteration. In crowd χ , the victory of lion i at iteration t is represented by:

$$Success(i, t, \chi) = \begin{cases} 1 & best_{i,\chi}^t < best_{i,\chi}^{t-1} \\ 0 & best_{i,\chi}^t = best_{i,\chi}^{t-1} \end{cases} \quad (7)$$

In Eq.(7), $best_{i,\chi}^t$ indicates the optimal locality discovered by i at t . The greatest count of victories defines that the lions boast convergence to a locality which is distant from the best locality. Likely, the least count of victories defines that the lions are fluctuating in the region of the best outcome with no enhancement. Therefore, it is utilized as the significant components for event range. Based on this success ranges, $K_j(sc)$ is computed by

$$K_j(sc) = \sum_{i=1}^n Success(i, t, \chi), j = 1, 2, \dots, \chi \quad (8)$$

In Eq.(8), n indicates the count of lions in a pride and $K_j(sc)$ refers to the count of lions in pride j that realizes a development in their objective during the final iteration. Thus, the event range in all prides is dynamic in all iterations. It defines if victory range minimizes, then event range is increased and thus the maximum diversity is achieved. Therefore, the event range is computed by Eq.(9):

$$T_j^{range} = \max \left(2, \text{ceil} \left(\frac{K_j(sc)}{2} \right) \right), j = 1, 2, \dots, \chi \quad (9)$$

Roaming

All male lions in a pride roam in that pride’s area owing to the number of causes. To imitate this characteristic of inhabitant males, %R of pride area are decided arbitrarily and are entered via that lion. Additionally, when inhabitant male enters a fresh locality stronger than its present optimal locality, his optimal entered outcome is modified. This wandering is a robust neighbouring hunt and helps lion optimizer to explore nearer outcome to develop it. To randomly search optimal space and mitigate trapping in local optima, nomad lions and their dynamic roaming are considered. So, the fresh locality of nomad lions is created as:

$$lion'_{ij} = \begin{cases} lion_{ij} & \text{if } rand_j > P_i \\ RAND_j & \text{or else} \end{cases} \quad (10)$$

In Eq.(10), $lion_{ij}$ is the present locality of i^{th} nomad lion and j^{th} range, $rand_j$ is a typical random number between 0 and 1, RAND is the arbitrary created vector in hunt space and P_i indicates the chance determined for all nomad lions separately by:

$$P_i = 0.1 + \min \left(0.5, \frac{(nomad_i - best_{nomad})}{best_{nomad}} \right), \quad i = 1, \dots, no.\ of\ nomad\ lions \quad (11)$$

In Eq.(11), $nomad_i$ and $best_{nomad}$ are the fitness of present locality of i^{th} lion in nomads and the optimal fitness of the nomad lions, correspondingly.

Mating

It is the essential procedure which ensures the lion’s survival and offers a chance for data transfer among members. In all prides, %Ma of female lions is mating with single or various inhabitant males. These males are decided randomly from identical pride as the female to create children. For nomad lions, it is varied that a nomad female merely mates with one of the males decided arbitrarily.

The mating operation is a linear fusion of parents to create 2 fresh children. Thus, the fresh cubs are created after deciding the female lion and males for mating as:

$$offspring,1 = \beta \times female\ lion_j + \sum_{i=1}^{NR} \frac{(1-\beta)}{Success_i} \times male\ lion_j^i \times Success_i \quad (12)$$

$$offspring,2 = (1-\beta) \times female\ lion_j + \sum_{i=1}^{NR} \frac{(\beta)}{Success_i} \times male\ lion_j^i \times Success_i \quad (13)$$

In Eq.(12) and Eq.(13) $Success_i$ is 1 when male i is decided for mating; or else, it is 0, NR indicates the count of inhabitant males in a pride, β refers to the arbitrarily produced integer with a regular distribution with an average 0.5 and standard variance 0.1. One of 2 fresh children is decided as male and another as female randomly. A metamorphosis is executed on all chromosomes of the created children having chance (%Mu). An arbitrary integer swaps the chromosome range. Through mating, lion optimizer distributes data between genders if fresh cubs come into behaviour from both sexual categories.

Resistance

Nomad male lions attack prides randomly to attack with another male in their pride. If the nomad lion is sufficiently powerful, the weakest male lion is rejected from the pride and called a nomad.

Migration

In all prides, the greatest number of females is computed using $\alpha\%$ of pride populace. For relocation function, few females decided arbitrarily and turned into nomads. The number of migrated females in all prides is equivalent to the addition of excess females in all prides and %I of the greatest count of females in a pride. If decided females relocate from prides and turn into nomad, fresh nomad females and previous nomad females are ordered depending on their objective. After, the optimal females amid them are decided arbitrarily and circulated

to prides for satisfying the unfilled locality of relocated females. It preserves the range of the entire populace and distributes data amid prides.

Lion's Generation Stability

Because there is constant stability in lion's populace, the number of lions must be controlled at the end of all iterations. Thus, the nomad lions with the minimum objective are discarded depending on the greatest allowed number of all genders in nomads.

This procedure is continued until the terminating condition is reached i.e., optimal set of L, α, τ, w , and k is obtained for each structure of MSDCNN model. Further, the MSDCNN is executed to extract the features at different scales i.e., kernel sizes and classify the ovarian tumor varieties.

Algorithm for DSSGL-EUNet-MSDCNN

Input: Ovarian tumor CT images

Output: Classified varieties of ovarian tumor

Begin

Collect the CT images from the TCGA-OV dataset;
Partition the entire dataset into training and testing sets;
for(training set)

Apply the DSSGL for augmenting the training CT images;
Learn EUNet to obtain the segmented feature map (ROI) for each CT image;

for(every ROI segment)

Learn the fused MSDCNN classifier by using the optimal hyperparameters;

//Hyperparameters selection process

Set initial L, α, τ, w , and k ;

Initialize the number of lions (MSDCNN structures) and the iterations t ;

Create a random solution for all lions;

Allocate prides and nomad lions;

while($t < t_{max}$) // t_{max} : Maximum iteration

for(each pride)

A number of female lions are decided randomly for hunting;

Remaining female lions move toward the best localities of the area;

All male lions roam in $\%R$ of area;

$\%Ma$ of female lions mate with only one inhabitant male lion;

Weakest male lion neglect from the pride and turn into the nomad;

for(each nomad lion)

Male and female lions move arbitrarily in the hunt space; $\%Ma$ of female lions mate with only single male lion;

Nomad male lions hit the prides;

for(each pride)

$\%I$ of female lions immigrate from the pride and turn into the nomad;

All genders of the nomad lion is sorted depending on their objective;

The optimal female lions are decided and spread to the prides for occupying the vacant localities;

Nomad lions with the minimum objective are neglected depending on the greatest allowed number of all genders;

end for

end for

end for

end while

Obtain the optimal set of optimal set of L, α, τ, w , and k for each network structure in the MSDCNN model;

end for

end for

Use the trained DSSGL-EUNet-MSDCNN fused structure classifier to categorize the testing CT images into different varieties of ovarian tumors;

End

4. EXPERIMENTAL RESULTS

In this section, the effectiveness of DSSGL-EUNet-MSDCNN model is evaluated by executing it in MATLAB 2017b using TCGA-OV dataset. From this dataset, 350 CT images (each ovarian tumor type contains 50 samples) are applied for training and 147 scans (each ovarian tumor type contains 21 samples) are applied for testing. The effectiveness comparison between proposed and existing models is conducted regarding different evaluation metrics. The existing models considered for analysis are DSSGL-EUNet-DCNN (Fusion) [9], DSSGL-DCNN (Fusion) [7], GSHPT [12], and Graph-cut-CNN [10].

4.1 ACCURACY

It is the percentage between a proper categorization of ovarian tumor types and the overall amount of tests performed Eq.(14)

$$Accuracy = (TP + TN) / (TP + TN + FP + FN) \quad (14)$$

True Positive (TP) is a solution where classifier classifies the ovarian tumor types as themselves e.g., serous carcinoma is categorized as serous carcinoma. True Negative (TN) is a solution where classifier classifies the healthy CT scans as healthy. False Positive (FP) is a solution where classifier improperly classifies the ovarian tumors as healthy. False Negative (FN) is a solution where classifier improperly classifies the healthy CT scans as any type of ovarian tumor.

The Fig.2 illustrates the accuracy attained by graph-cut-CNN, GSHBT, DSSGL-DCNN (fusion), DSSGL-EUNet-DCNN (fusion), and DSSGL-EUNet-MSDCNN (fusion) frameworks for categorizing the varieties of ovarian tumor. It indicates that the DSSGL-EUNet-MSDCNN (fused structure) model increases accuracy compared to all other models for e.g., the accuracy of DSSGL-EUNet-MSDCNN (fusion) is 8.49% greater than the graph-cut-CNN, 7.83% greater than the GSHBT, 6.91% better than the DSSGL-DCNN (fusion) and 2.39% better than the DSSGL-EUNet-DCNN (fusion) frameworks.

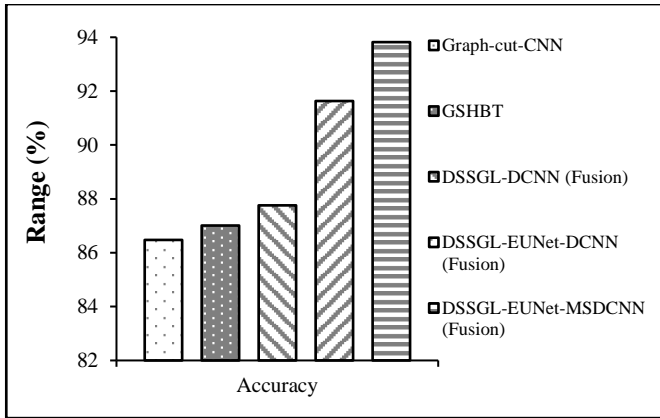


Fig.2. Analysis of Accuracy

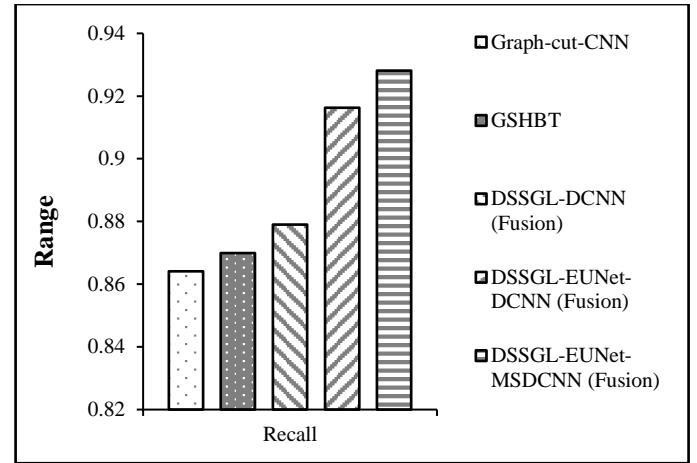


Fig.4. Analysis of Recall

4.2 PRECISION

It defines the percentage of properly categorized ovarian tumor varieties at TP and FP rates Eq.(15),

$$\text{Precision} = \frac{\text{No. of properly categorized @ ovarian tumor types}}{\text{No. of properly categorized ovarian tumortypes + @No. of improperly categorized ovarian tumor types}} \quad (15)$$

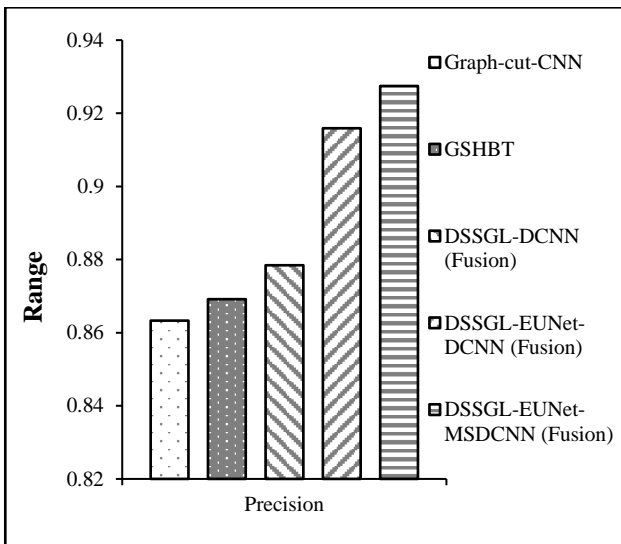


Fig.3. Analysis of Precision

The Fig.3 shows the precision attained by graph-cut-CNN, GSHBT, DSSGL-DCNN (fusion), DSSGL-EUNet-DCNN (fusion), and DSSGL-EUNet-MSDCNN (fusion) models. It addresses that the DSSGL-EUNet-MSDCNN (fused structure) model improves the precision compared to all other models for e.g., the precision of DSSGL-EUNet-MSDCNN (fusion) is 7.44% greater than the graph-cut-CNN, 6.71% greater than the GSHBT, 5.59% superior to the DSSGL-DCNN (fusion), and 1.27% superior to the DSSGL-EUNet-DCNN (fusion) frameworks.

4.3 RECALL

It is the percentage of properly categorized ovarian tumor varieties at TP and FN rates Eq.(16).

$$\text{Recall} = \frac{\text{No. of properly categorized @ ovarian tumor types}}{\text{No. of properly categorized ovarian tumor types + @No. of improperly categorized ovarian tumor types}} \quad (16)$$

The Fig.4 depicts the recall attained by graph-cut-CNN, GSHBT, DSSGL-DCNN (fusion), DSSGL-EUNet-DCNN (fusion), and DSSGL-EUNet-MSDCNN (fusion) models. It notices that the DSSGL-EUNet-MSDCNN (fused structure) model enhances the recall compared to all other models for e.g., the recall of DSSGL-EUNet-MSDCNN (fusion) is 7.41% larger than the graph-cut-CNN, 6.69% larger than the GSHBT, 5.59% larger than the DSSGL-DCNN (fusion), and 1.29% larger than the DSSGL-EUNet-DCNN (fusion) models.

4.4 F-MEASURE

It defines the harmonic average of precision and recall.

$$F\text{-measure} = \frac{2 \times (\text{Precision} \cdot \text{Recall})}{(\text{Precision} + \text{Recall})} \quad (17)$$

Fig.5 exhibits the f-measure attained by various models such as graph-cut-CNN, GSHBT, DSSGL-DCNN (fusion), DSSGL-EUNet-DCNN (fusion), and DSSGL-EUNet-MSDCNN (fusion) models. It refers to that the DSSGL-EUNet-MSDCNN (fused structure) model increases the f-measure compared to all other frameworks, i.e., the f-measure of DSSGL-EUNet-MSDCNN (fusion) is 7.42% superior to the graph-cut-CNN, 6.71% superior to the GSHBT, 5.59% superior to the DSSGL-DCNN (fusion) and 1.28% superior to the DSSGL-EUNet-DCNN (fusion) models.

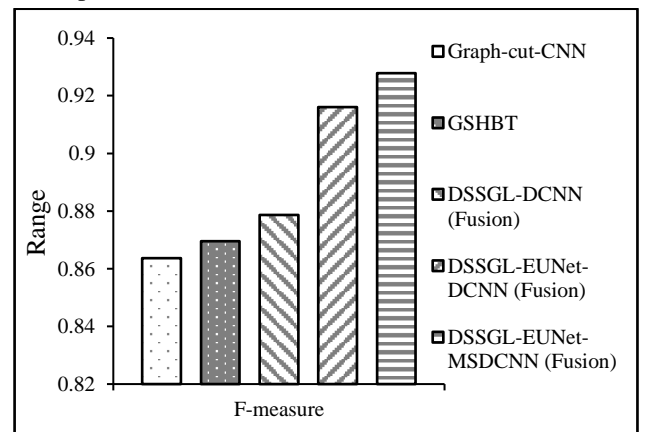


Fig.5. Analysis of F-measure

5. CONCLUSION

In this article, the DSSGL-EUNet-MSDCNN model was presented to optimize the learning variables and classify the ovarian tumor types. At first, the DSSGL was used to augment the training CT scans and the EUNet model was used to segment the ROIs from each CT scan. After, these ROIs were given to the MSDCNN fused structure. In this MSDCNN, the number of layers, dropout rate, learning rate, weights, and kernel sizes for each network structure were optimized by the lion optimization algorithm which lessens the training errors. So, the features from all ROIs were extracted and classified at a scale-level for recognizing the ovarian tumor types. Finally, the findings proved that the DSSGL-EUNet-MSDCNN model achieves 93.82% of accuracy compared to the other models for segmenting and classifying the ovarian tumor types.

REFERENCES

- [1] S.H. Rosenthal, A. Gerasimova, C. Ma, H.R. Li, A. Grupe, H. Chong and F. Lacbawan, "Analytical Validation and Performance Characteristics of a 48-Gene Next-Generation Sequencing Panel for Detecting Potentially Actionable Genomic Alterations in Myeloid Neoplasms", *Plos One*, Vol. 16, No. 4, pp. 1-21, 2021.
- [2] S. Bhattacharjee, Y.J. Singh and D. Ray, "Comparative Performance Analysis of Machine Learning Classifiers on Ovarian Cancer Dataset", *Proceedings of IEEE 3rd International Conference on Research in Computational Intelligence and Communication Networks*, pp. 213-218, 2017.
- [3] J. Liu, H. Meng, S. Li, Y. Shen, H. Wang, W. Shan and W. Cheng, "Identification of Potential Biomarkers in Association with Progression and Prognosis in Epithelial Ovarian Cancer by Integrated Bioinformatics Analysis", *Frontiers in Genetics*, Vol. 10, pp. 1-37, 2019.
- [4] S. Rizzo, L. Manganaro, M. Dolciemi, M.L. Gasparri, A. Papadia and F. Del Grande, "Computed Tomography based Radiomics as a Predictor of Survival in Ovarian Cancer Patients: A Systematic Review", *Cancers*, Vol. 13, No. 3, pp. 1-11, 2021.
- [5] B. Levine and C. Schlosser, J. Grewal, R. Coope, S.J. Jones and S. Yip, "Rise of the Machines: Advances in Deep Learning for Cancer Diagnosis", *Trends in Cancer*, Vol. 5, No. 3, pp. 157-169, 2019.
- [6] Y. Zhang, J. M. Gorriz and Z. Dong, "Deep Learning in Medical Image Analysis", *Journal of Imaging*, Vol. 7, pp. 1-4, 2021.
- [7] N. Pillai Honey and N. Tajunisha, "Automatic Classification of Ovarian Cancer Types from CT Images using Deep Semi-Supervised Generative Learning and Convolutional Neural Network", *Revue d'Intelligence Artificielle*, Vol. 35, No. 4, pp. 273-280, 2021.
- [8] O. Ronneberger, P. Fischer and T. Brox, "U-Net: Convolutional Networks for Biomedical Image Segmentation", *Proceedings of International Conference on Medical Image Computing and Computer-Assisted Intervention*, pp. 234-241, 2015.
- [9] N. Pillai Honey and N. Tajunisha, "Automatic Classification of Ovarian Cancer Types from CT Images Using Deep SemiSupervised Generative Learning and Convolutional Neural Network", *Revue d'Intelligence Artificielle*, Vol. 35, No. 4, pp. 273-280, 2021.
- [10] P. Nardelli, D. Jimenez-Carretero, D. Bermejo-Pelaez, G.R. Washko, F.N. Rahaghi, M.J. Ledesma-Carbayo and R.S.J. Estepar, "Pulmonary Artery-Vein Classification in CT Images using Deep Learning", *IEEE Transactions on Medical Imaging*, Vol. 37, No. 11, pp. 2428-2440, 2018.
- [11] J. Tan, Y. Gao, Z. Liang, W. Cao, M.J. Pomeroy, Y. Huo and P.J. Pickhardt, "3D-GLCM CNN: A 3-Dimensional Gray-Level Co-Occurrence Matrix-based CNN Model for Polyp Classification via CT Colonography", *IEEE Transactions on Medical Imaging*, Vol. 39, No. 6, pp. 2013-2024, 2019.
- [12] B.H. Shekar and G. Dagnew, "Grid Search-Based Hyperparameter Tuning and Classification of Microarray Cancer Data", *Proceedings of IEEE Second International Conference on Advanced Computational and Communication Paradigms*, pp. 1-8, 2019.
- [13] M.I. Georgescu, R.T. Ionescu and N. Verga, "Convolutional Neural Networks with Intermediate Loss for 3D Super-Resolution of CT and MRI Scans", *IEEE Access*, Vol. 8, pp. 49112-49124, 2020.
- [14] X. Qian, H. Fu, W. Shi and T. Chen, Y. Fu, F. Shan and X. Xue, "M³Lung-Sys: A Deep Learning System for Multi-Class Lung Pneumonia Screening from CT Imaging", *IEEE Journal of Biomedical and Health Informatics*, Vol. 24, No. 12, pp. 3539-3550, 2020.
- [15] H. Yaghoobi, E. Babaei, B.M. Hussen and A. Emami, "EBST: An Evolutionary Multi-Objective Optimization based Tool for Discovering Potential Biomarkers in Ovarian Cancer", *IEEE/ACM Transactions on Computational Biology and Bioinformatics*, Vol. 18, No. 6, pp. 1-11, 2020.
- [16] S.K. Prabhakar and S.W. Lee, "An Integrated Approach for Ovarian Cancer Classification with the Application of Stochastic Optimization", *IEEE Access*, Vol. 8, pp. 127866-127882, 2020.